King Saud University

Arabian Journal of Chemistry

ORIGINAL ARTICLE

Arylnaphthalide lignans from *Saussurea medusa* and their anti-inflammatory activities

Jing-Ya Cao [a,b], **Qi Dong** [a], **Zhi-Yao Wang** [c], **Ye Zhao** [d], **Yu Ren** [d], **Chang Liu** [d], **Jun Dang** [a], **Rui-Tao Yu** [a,*], **Yan-Duo Tao** [a,*]

[a] *Qinghai Provincial Key Laboratory of Tibetan Medicine Research, Key Laboratory of Tibetan Medicine Research, Northwest Institute of Plateau Biology, Chinese Academy of Sciences, Xining 810008, PR China*
[b] *University of Chinese Academy of Sciences, No. 19A Yuquan Road, Beijing 100049, PR China*
[c] *Henan Academy of Science, Zhengzhou 450002, PR China*
[d] *State Key Laboratory of Drug Research, Shanghai Institute of Materia Medica, Chinese Academy of Sciences, 555 Zuchongzhi Road, Shanghai 201203, PR China*

Abstract Five new arylnaphthalide lignans (1 − 4a/4b), together with five known analogues (5–9), were isolated from whole plants of *Saussurea medusa*. Compound 4 was characterized as an aryltetralin lignan with an unusual C-7′-C-9 oxygen bridge group, and a chiral HPLC analysis was carried out to afford one pair of enantiomers (4a/4b). Structures of the new compounds were elucidated by extensive spectroscopic and electronic circular dichroism (ECD) calculations. All compounds were firstly isolated from *S. medusa*, and compounds 1–5, 7 and 8 had never been obtained from the genus *Saussurea* previously. Furthermore, this is the first report of arylnaphthalide lignans isolated from *S. medusa*. anti-inflammatory activities of the compounds were evaluated by determining their inhibitory activities on the production of NO by LPS-stimulated RAW 264.7 cells. Compounds (−)-4a and 5 exerted the significant inhibition activities with IC_{50} values of 13.4 ± 1.5 and 15.7 ± 1.1 μM, respectively, which even exceeded the positive control quercetin (IC_{50} = 15.9 ± 1.2 μM). Compounds 2, (+)-4b, 6 and 9 exhibited moderate inhibitory activities with IC_{50} values ranging from 19.7 ± 1.9 to 47.4 ± 3.1 μM. Further analysis by molecular docking showed that almost all the active compounds could interact with the amino acid residues of iNOS proteins, which also supported their anti-inflammatory activities.

* Corresponding authors at: Northwest Institute of Plateau Biology, Chinese Academy of Sciences, Xining, PR China.
 E-mail addresses: yuruitao@nwipb.cas.cn (R.-T. Yu), tyd@nwipb.cas.cn (Y.-D. Tao).

Production and hosting by Elsevier
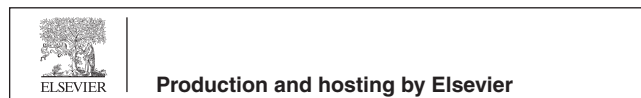
1. Introduction

Inflammation represents the basis of severe acute and chronic syndromes like rheumatic arthritis (Selmi et al., 2014), inflammatory bowel disease (Wang et al., 2014), Parkinson's disease (Su and Federoff, 2014) and cancer (Hagerling et al., 2015). Nitric oxide (NO), a gaseous free radical, has been identified as an important molecule involved in immune responses and inflammation (Guzik et al., 2003). NO is produced by inducible nitric oxide synthase (iNOS) in macrophages, hepatocytes, and renal cells, under stimulation of lipopolysaccharide (LPS) (Cuong et al., 2012), higher concentrations of NO synthesized by iNOS is essential in inflammation and the related processes (Aktan, 2004). Therefore, it is important to obtain optically pure compounds and evaluate their inhibitory effects of NO production to provide a strategy for the treatment of inflammatory diseases.

Saussurea medusa (Asteraceae), a rare subnival plant known as "snow lotus", is mainly distributed in the Qinghai-Tibet plateau at heights of 3500–4500 m. S. medusa is a very important, but endangered, traditional Chinese medicinal herb used for the treatment of rheumatic arthritis, menoxenia, gynopathy, traumatic bleeding, anthrax, febrile tingling and headache (Fan and Yue, 2003; Xie et al., 2005). Our previous study showed that the alcohol extract of S. medusa had anti-inflammatory effect against LPS-induced acute lung injury mice (Yu et al., 2019). In an attempt to find novel anti-inflammatory compounds from S. medusa, an ethanol extract of S. medusa had been investigated.

Arylnaphthalene lignans are common in natural products, mainly exist in the plants of family Berberidaceae, Angiospermae, Burseraceae, Verbenaceae, Euphorbiaceae, etc (Sun et al., 2013). Taking podophyllotoxin as an example, arylnaphthalene lignans exhibited an array of biological activities, such as antifungal, antiprotozoal, cytotoxic and anti-inflammatory effects (Day et al., 2000; Gertsch et al., 2003; Tuchinda et al., 2005). Owing to their promising broad spectrum of bioactivities and the potential druggability, they have become hot research topics in drug research. To data, however, the most common recorded lignans in S. medusa were dibenzylbutyrolactone and tetrahydrofuran lignans (Fan et al., 2015; Duan et al., 2002; Xie et al., 2005). As far as we know, arylnaphthalide lignans had not been reported in S. medusa.

As a result of our ongoing phytochemical investigation on S. medusa, five new arylnaphthalide lignans (1 − 4a/4b), including one pair of enantiomers (4a/4b), together with five known analogues (5–9), were isolated from whole plants of S. medusa. Extensive spectroscopic data and time-dependent density functional theory-based electronic circular dichroism (TDDFT-ECD) calculation (Pescitelli and Bruhn, 2016) had led to assignments of configurations for the new compounds. anti-inflammatory activities of the compounds were evaluated by determining their inhibitory activities on the production of NO by LPS-stimulated RAW 264.7 cells.

Molecular docking is the most accurate method for predicting the modus of drug-receptor interactions in silico (Azam et al., 2012). This technique is routinely used to accelerate the recognition and investigation of novel drug candidates (Hussain et al., 2022). In this study, molecular docking was conducted to investigate the interactions between the bioactive compounds and iNOS proteins to explore the possible mechanism of inhibiting NO production.

Hence, this research investigated the isolation, structural characterization, anti-inflammatory effects and their possible mechanism researches of the arylnaphthalide lignans from S. medusa.

2. Materials and methods

2.1. General experimental procedures

Optical rotations (Na lamp, 589 nm) were carried out on an Autopol VI automatic polarimeter at room temperature. UV spectra were recorded on a Shimadzu UV-2550 UV–visible spectrophotometer. ECD spectra were obtained on a JASCO J-815 spectrometer using a 0.1 cm path length sample cell and JASCO LC-J1500 consisting of a MD-4014 photo diode array detector, an AS-4050 HPLC auto sampler, a PU-4185 binary and a CO-4060 column oven. IR spectra were measured on a Thermo IS5 spectrometer with KBr panels. NMR spectra were acquired on a Bruker Avance III 600 MHz spectrometer (Bruker Biospin AG, Switzerland) with TMS as an internal standard. (±)-ESIMS and (±)-HRESIMS analysis were performed on a Bruker Daltonics Esquire 3000 Plus LC-MS instrument and a Waters Q-TOF Ultima mass spectrometer, respectively. Silica gel (200–300 and 300–400 mesh, Qingdao Haiyang Chemical Co. ltd.), C18 reversed-phase silica gel (150–200 mesh, Merck), MCI gel (CHP20P, 75–150 μm, Mitsubishi Chemical Industries, ltd.) and Sephadex LH-20 (GE Healthcare, Uppsala, Sweden) were used for column chromatography (CC). Precoated silica gel GF254 plates (Qingdao Haiyang Chemical Co. ltd.) were used for TLC detection. Semipreparative HPLC was carried out on a Waters 2695 binary pump system with a Waters 2489 detector (210 and 254 nm) using a YMC-Pack ODS-A column (250 × 10 mm, S-5 μm) or a Waters X-Bridge Prep C18 column (250 × 10 mm, S-5 μm). All solvents were of analytical grade (Shanghai Chemical Reagents Co. ltd., China), and solvents used for HPLC were of HPLC grade (J & K Scientific ltd., China).

2.2. Plant material

The whole plants of S. medusa were collected from Yeniu Ditch (altitude 4100 m), Qilian County, Xining City, Qinghai Province in August 2018, and were identified by Professor Lijuan Mei. The specimen was kept in the Key Laboratory of Tibetan Medicine of the Chinese Academy of Sciences (access number: 0341202).

2.3. Extraction and isolation

The air-dried and powdered whole herbs of S. medusa (15.0 kg) were soaked overnight and then extracted three times with 75 L of 95 % EtOH at an ambient temperature for 12 h to obtain the crude extract (800.7 g). This extract was then suspended in water (4 L) and successively partitioned with petroleum ether (5 × 4 L), EtOAc (5 × 4 L) and n-butanol (5 × 4 L). The EtOAc-soluble fraction (90.1 g) was subjected to a column of MCI gel eluted with MeOH-H_2O (10 % to 100 %) to give fractions F1-F7 based on TLC analysis. Fraction F3 (8.3 g) was subjected to a silica gel column eluted with CH_2Cl_2/MeOH (400:1 to 1:1) in gradient to give subfractions F3a-F3k. Separation of F3g (0.9 g) with Sephadex LH-20 (MeOH) and RP semi-preparative HPLC (25 % MeOH in H_2O), successively, yielded 1 (13 mg) and 2 (6 mg). Similarity, F3h (0.8 g) was separated over a Sephadex LH-20 column eluted with MeOH and purified by semi-preparative HPLC with 24 % MeOH in H_2O to afford 9 (16 mg). Fraction F5 (26.4 g) was chromatographed over a silica gel column eluted with CH_2Cl_2/MeOH (400:1 to 10:1) in gradient to yield fractions F5a-F5g. Fraction F5a (0.7 g) was separated over a Sephadex LH-20 column eluted with EtOH to afford subfractions F5a1-F5a3. Fraction F5a3 (108 mg) was then purified by semi-preparative HPLC with

50 % MeOH in H_2O as the mobile phase to afford compounds **3** (2 mg) and **4** (7 mg). F5f (1.6 g) was fractioned via Sephadex LH-20 (MeOH) to afford subfractions F5f1-F5f7. Fraction F5f3 (501 mg) was subjected to a silica gel column eluted with CH_2Cl_2/MeOH (400:1 to 1:1) in gradient to give subfractions F5f31-F5f38. F5f35 (66 mg) was then separated over a Sephadex LH-20 (EtOH) and followed by RP semi-preparative HPLC (42 % MeOH in H_2O) purification to yield **5** (5 mg) and **6** (15 mg). Fraction F4 (15.8 g) was subjected to a silica gel column eluted with CH_2Cl_2/MeOH (400:1 to 1:1) in gradient to give subfractions F4a-F4k. Separation of F4k (1.0 g) with Sephadex LH-20 (MeOH) yielded subfractions F4k1-F4k3. Fraction F4k2 (243 mg) was subjected to a silica gel column eluted with *n*-hexane/isopropanol (80:1 to 1:1) in gradient to give subfractions F4k21-F4k23. F4k21 (87 mg) was then purified by RP semi-preparative HPLC (32 % MeOH in H_2O) to yield **7** (7 mg) and **8** (14 mg).

2.4. Details of new compounds

2.4.1. Saumedin A (*1*)

White amorphous solid; $[\alpha]_D^{25}$ − 100.3 (*c* 0.33 in MeOH); ^1H and ^{13}C NMR (CD_3OD) data, see Table 1; IR (KBr) v_{max} 3363, 2924, 2852, 1660, 1601, 1514, 1464, 1428, 1384, 1270, 1125, 1056, 1032 cm^{-1}; UV (MeOH) λ^{max} (log ε) 233 (3.10), 284 (2.88); CD (MeOH) λ ($\Delta\varepsilon$) 212 (−18.58), 239 (−12.02), 275 (−4.61), 292 (+0.73) nm; (+)-ESIMS *m/z* 399.9 [M + Na]$^+$; (−)-HRESIMS *m/z* 375.1449 [M − H]$^-$ (calcd for $C_{20}H_{23}O_7$, 375.1449).

2.4.2. Saumedin B (*2*)

White amorphous solid; $[\alpha]_D^{25}$ − 12.3 (*c* 0.30 in MeOH); ^1H and ^{13}C NMR (CD_3OD) data, see Table 1; IR (KBr) v_{max} 3359, 3194, 2922, 2851, 1660, 1633, 1513, 1468, 1422, 1384, 1277, 1134, 1035 cm^{-1}; UV (MeOH) λ^{max} (log ε) 230 (3.40), 282 (3.08); CD (MeOH) λ ($\Delta\varepsilon$) 209 (−9.21), 238 (+4.48), 271 (+3.06), 290 (−12.14) nm; (−)-ESIMS *m/z* 375.2 [M − H]$^-$; (+)-HRESIMS *m/z* 399.1421 [M + Na]$^+$ (calcd for $C_{20}H_{24}$-NaO_7, 399.1414).

2.4.3. Saumedin C (*3*)

Light yellow amorphous solid; ^1H and ^{13}C NMR (CD_3OD) data, see Table 1; IR (KBr) v_{max} 3418, 2927, 1748, 1602, 1515, 1433, 1261, 1097, 1032 cm^{-1}; UV (MeOH) λ^{max} (log ε) 228 (3.68), 266 (3.81), 308 (3.21), 355(2.92); (+)-ESIMS *m/z* 383.3 [M + H]$^+$; (−)-ESIMS *m/z* 381.3 [M − H]$^-$; (+)-HRESIMS *m/z* 383.1126 [M + H]$^+$ (calcd for $C_{21}H_{19}O_7$, 383.1125).

2.4.4. Saumedin D (*4*)

Light yellow gum; $[\alpha]_D^{25}$ + 1.4 (*c* 0.3 in MeOH); ^1H and ^{13}C NMR ($CDCl_3$) data, see Table 1; IR (KBr) v_{max} 3422, 2936, 1736, 1602, 1514, 1464, 1370, 1272, 1117, 1035 cm^{-1}; UV (MeOH) λ^{max} (log ε) 234 (3.44), 285 (3.14); (−)-ESIMS *m/z* 399.2 [M − H]$^-$; (+)-HRESIMS *m/z* 423.1411 [M + Na]$^+$ (calcd for $C_{22}H_{24}NaO_7$, 423.1414).

4a: light yellow gum; $[\alpha]_D^{25}$ − 31.3 (*c* 0.2 in MeOH); CD (MeOH) λ ($\Delta\varepsilon$) 215 (−41.85), 245 (+17.21), 275 (+4.87), 292 (−10.57) nm;

4b: light yellow gum; $[\alpha]_D^{25}$ + 34.1 (*c* 0.2 in MeOH); CD (MeOH) λ ($\Delta\varepsilon$) 213 (+43.22), 245 (−12.00), 275 (−4.40), 292 (+10.15) nm;

2.5. Chiral HPLC analysis of compound 4

Chiral HPLC analysis was performed using a Waters 2695 liquid chromatography system on five parallel connected chiral columns (250 × 4.6 mm, S-5 μm). Column 1: CHIR-ALPAK AD-H (Lot No. ADH0CE-NL030 Part No 19325); Column 2: CHIRALPAK IA (Lot No. IA00CE-AO016 Part No 80325); Column 3: CHIRALPAK IC (Lot No. IC00CE-AP062 Part No 83325); Column 4: CHIRALPAK IG (Lot No. IG00CE-AN006 Part No 87325); Column 5: CHIRALPAK IH (Lot No. IH00CE-AX011 Part No 89325). Mobile phase: (A) *n*-hexane (B) isopropanol. Column temperature: 30 °C. Flow rate: 1.0 mL/min. Injection volume: 3 μL. Eluted compounds were detected using a Waters 2998 PDA detector with a wavelength range of λ = 200–400 nm.

2.6. ECD calculations for 1, 2 and 4

The absolute configurations of **1**, **2** and **4** were determined by quantum chemical TDDFT calculations of their theoretical ECD spectra. Using the MM2 force field in the Chem3D pro 14.0 software, the initial conformers of each compound were established. Conformational searches were conducted with the torsional sampling method (Monte Carlo Multiple Minimum, MCMM) under OPLS3 (Harder et al., 2015) force field by Maestro 11.5 software (Maestro Technologies, Inc., Trenton, NJ, USA) in an energy window of 12.6 kJ/mol. The conformational optimization and the following TDDFT calculations for the conformers that satisfied the experiment coupling constants and NOE signals were all carried out with the Gaussian 16 program package (Frisch et al., 2016) at the B3LYP/6-31G(d) level in methanol. All TDDFT calculations were computed at the PCM/ωB97XD/6-311G** level of theory in methanol. Finally, the Boltzmann-averaged ECD spectra were simulated with SpecDis 1.71 (Bruhn et al., 2013; Pescitelli and Bruhn, 2016).

2.7. Determination of NO production and cell viability assay

Measurements of NO production in an activated macrophage-like cell line as described previously (Cuong et al., 2012). Briefly, RAW 264.7 cells (1×10^5 cells/well) were cultured in 96-well plates with DMEM high-glucose medium supplemented with 10 % fetal bovine serum (FBS), 2.0 mM glutamine, 1 mM pyruvate, 10.0 μg/mL of streptomycin and 100.0 U/mL of penicillin at 37 °C in a humidified atmosphere with 5 % CO_2. The cells were treated with 1.0 μg/mL of LPS and with the test compounds (3.125, 6.25, 12.5, 25.0 and 50.0 μM) for 24 h. Absorbance was measured at 540 nm after incubating culture media (100 μL/each well) with Griess reagent (100 μL) (Sigma-Aldrich, St. Louis, MO, USA) at room temperature. The concentration of NO was calculated using a $NaNO_2$ solution standard. Cell viability was measured using the MTT assay.

Table 1 ^{1}H NMR (400 MHz) and [13]C (125 MHz) Data for Compounds 1–4 (δ_H in ppm, J in Hz).

position	1[a] δ_C, type	1[a] δ_H (J in Hz)	3[a] δ_C, type	3[a] δ_H (J in Hz)	4[b] δ_C, type	4[b] δ_H (J in Hz)
1	135.6, C	—	128.3, C	—	134.8, C	—
2	115.5, CH	6.76, d (1.2)	115.7, CH	6.90, d (1.8)	111.9, CH	6.61, d (1.7)
3	148.3, C	—	148.6, C	—	146.4, C	—
4	146.1, C	—	147.3, C	—	144.3, C	—
5	115.4, CH	6.65, d (8.1)	115.9, CH	6.93, d (8.0)	114.2, CH	6.86, d (8.1)
6	124.1, CH	6.51, dd (8.1, 1.2)	124.5, CH	6.77, dd (8.0, 1.8)	122.5, CH	6.67, dd (8.1, 1.7)
7	54.4, CH	4.03, s	132.8, C	—	46.2, CH	4.40, d (4.5)
8	76.3, C	—	123.0, C	—	43.6, CH	2.61, q-like (4.5)
9	67.3, CH$_2$	a 3.55, d (11.2) b 3.34, d (11.2)	173.0, C	—	68.4, CH$_2$	α 3.92, overlap β 3.68, dd (8.7, 4.5)
1′	127.9, C	—	125.6, C	—	129.8, C	—
2′	112.1, CH	6.72, s	101.9, CH	7.68, s	110.1, CH	6.65, s
3′	147.8, C	—	152.3, C	—	145.3, C	—
4′	145.7, C	—	151.4, C	—	145.7, C	—
5′	117.8, CH	6.32, s	107.4, CH	7.10, s	115.8, CH	6.65, s
6′	131.8, C	—	131.8, C	—	129.2, C	—
7′	30.1, CH$_2$	α 2.88, dd (17.0, 6.5) β 2.80, dd (17.0, 10.5)	146.6, C	—	77.9, CH	4.69, d (4.8)
8′	38.5, CH	2.29, m	119.6, C	—	44.5, CH	2.79, m
9′	63.4, CH$_2$	a 3.77, overlap b 3.58, dd (10.5, 5.0)	68.2, CH$_2$	5.37, s	62.1, CH$_2$	a 4.28, dd (11.3, 7.1) b 4.02, dd (11.3, 7.7)
10′					171.0, C	—
11′					20.9, CH$_3$	2.09, s
OMe-3/3′	56.4, CH$_3$/56.4, CH$_3$	3.77, s/3.83, s	56.6, CH$_3$ /56.3, CH$_3$	3.84, s/4.01, s	56.0, CH$_3$/56.1, CH$_3$	3.81, s/3.90, s
OMe-4′/5′			56.0, CH$_3$ /	3.72, s/		
4-OH/4′-OH						5.55, s/5.54, s

[a] Measured in CD$_3$OD.
[b] Measured in CDCl$_3$.

2.8. Molecular docking study

Chemical structures of active compounds were drawn using the ChemDraw program and converted to their three-dimensional (3D) coordinates in Chem3D. Each of them was subjected to energy minimization by the MM2 method and saved in "sdf" format. The 3D crystal structure of iNOS (PDB ID: 3E6T) was obtained from the RCSB Protein Data Bank (https://www.rcsb.org/pdb) (Zhang et al., 2019) and handled in Biovia Discovery Studio Visualizer 2020 program for checking any missing residue/atom and deleting co-crystallized molecules such as cofactors, inhibitors, and water. The proteins and ligands were processed by AutoDock-Tools 1.5.6 and converted to "pdbqt" format. The grid box was set to contain the whole molecule. The docked model with the lowest docking energy was selected to represent its most favorable binding pattern, with prediction performed using AutoDock Vina.

3. Results and discussion

3.1. Isolation and identification of compounds

The ethyl acetate fraction of whole herbs of *S. medusa* was subjected to repeated chromatographic methods, which yielded a lignan-enriched fraction. Further purification of this fraction afforded five new arylnaphthalide lignans, namely saumedin A − D (1 − 4a/4b), see Fig. 1.

Saumedin A (1) had a molecular formula of C$_{20}$H$_{24}$O$_7$ on the basis of an (−)-HRESIMS ion at m/z 375.1449 [M − H]$^-$ (calcd for C$_{20}$H$_{23}$O$_7$, 375.1449) with nine indices of hydrogen deficiency (IHDs). Its IR spectrum showed absorption bands consistent with the presence of hydroxy (3363 cm^{-1}) and aromatic ring (1601, 1514, and 1032 cm^{-1}) functionalities. The ^{1}H NMR spectrum (Table 1) of 1 showed an aromatic ABX coupling system characteristic of a group of protons at δ_H 6.76 (1H, d, J = 1.2 Hz, H-2), 6.65 (1H, d, J = 8.1 Hz, H-5) and 6.51 (1H, dd, J = 8.1, 1.2 Hz, H-6), suggesting the presence of one 1,2,4-trisubstituted aromatic ring. Two singlet aromatic protons at δ_H 6.72 (1H, s, H-2′) and 6.32 (1H, s, H-5′) indicated the existence of one 1,2,4,5-tetrasubstituted aromatic ring. In addition, two methoxy groups at δ_H 3.77 (3H, s, 3-O*Me*) and 3.83 (3H, s, 3′-O*Me*) were also observed. The ^{13}C NMR (Table 1) and DEPT spectra showed 20 carbon signals, consisting of 12 aromatic carbons (δ_C 112.1–148.3), three methylenes (δ_C 30.1, two oxygenated at δ_C 63.4, 67.3), two methines (δ_C 38.5, 54.4), two methoxys at δ_C 56.4 (overlapped) and one oxygenated quaternary carbon at δ_C 76.3.
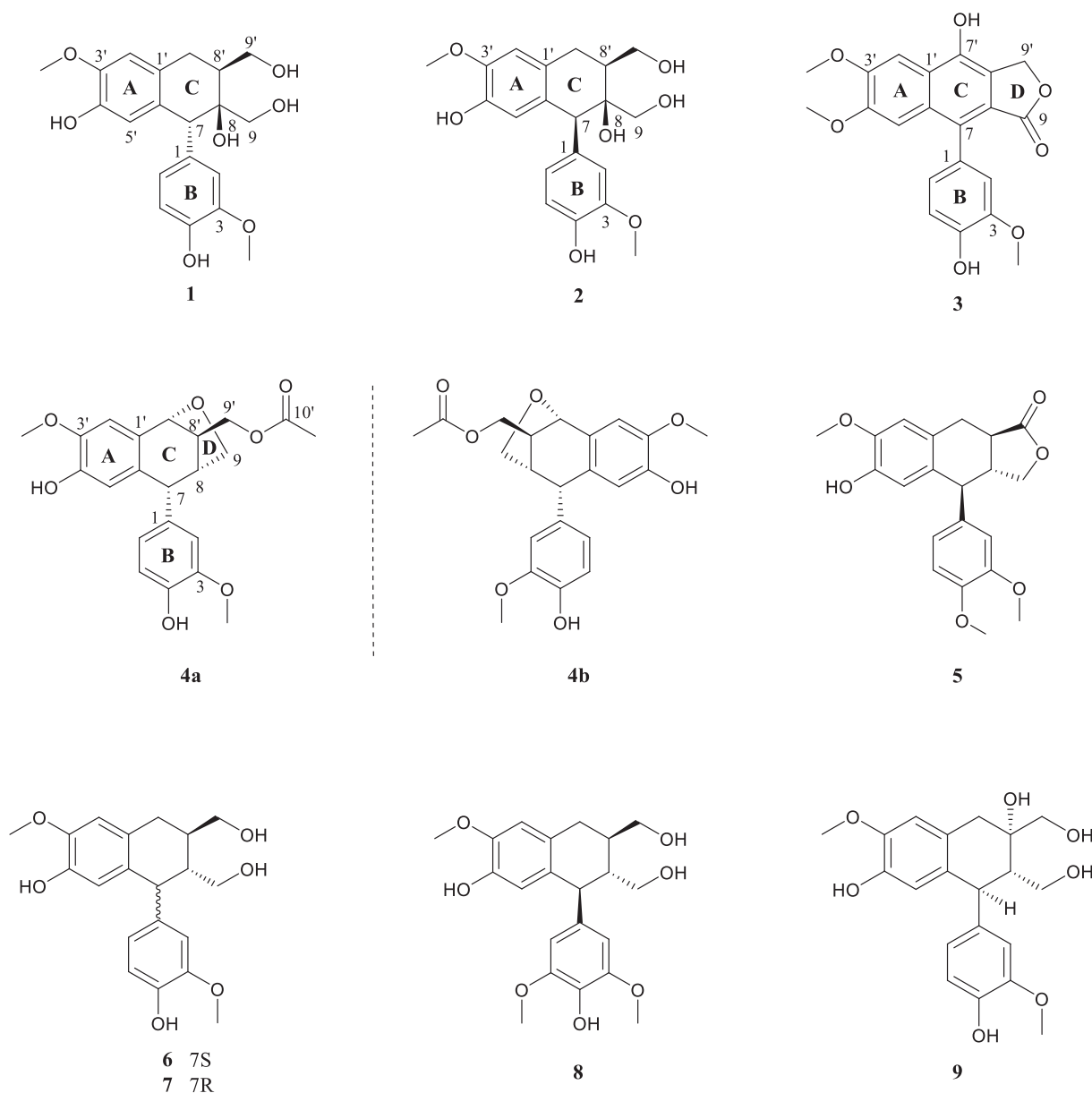
Fig. 1 Chemical structures of compounds 1–9.

Two aromatic rings (A and B) accounted for eight out of nine IHDs, and the remaining one IHD in the molecule implied that **1** was likely a tricyclic aryltetralin lignan skeleton. The 1,2,4,5-tetrasubstituted aromatic ring A was assigned based on the HMBC correlations (Fig. 2) of H-2′/C-4′ and C-6′; and H-5′/C-1′ and C-3′. The position of a methoxy group (δ_H 3.83) was assigned to be at C-3′ due to its HMBC correlation to C-3′. Similarly, the 1,2,4-trisubstituted aromatic ring B was determined by the HMBC correlations from H-6 to C-2 and C-4; and from H-5 to C-1 and C-3. The HMBC correlations of 3-O*Me*/C-3 located a methoxy at C-3. The two aromatic rings (A and B) were connected by a hexatomic ring C, which was deduced from the HMBC correlations of H_2-7′/C-2′, C-6′ and C-8; and H-7/C-5′, C-1, C-2 and C-6. Meanwhile, ^{1}H$-^1$H COSY correlations (Fig. 2) of H_2-7′/H-8/H_2-9′ led to the establishment of a spin coupling unit, which also supported the 7-aryltetralin lignan skeleton. By comparison

with literature data, compound **1** was found to be similar to (+)-cycloolivil (Bai et al., 2015), a known compound (**9**) also isolated from this plant in this research, with the obvious difference that the C-8′ hydroxy in (+)-cycloolivil was migrated to C-8 position in **1**. This conclusion was deduced by the singlet proton peak of H-7 δ_H 4.03 (1H, s), as verified by the ^{1}H$-^1$H COSY correlations of H_2-7′/H-8′/H_2-9′.

The relative stereochemistry at C-7, C-8, and C-8′ in **1** was determined by means of ROESY correlations (Fig. 3). The key cross-peak of H-8′ and H_2-9 suggested that they were spatially vicinal and assigned arbitrarily in an α-orientation. The aromatic group at C-7 was assigned as an α-orientation based on the ROESY correlations between H-2, H-6 and H-9b. Therefore, the relative configuration of **1** was determined to be 7*R**,8*S**,8′*S**.

A review of ECD data by Ayres and Loike (Ayres and Loike, 1990; Tran et al., 2016) indicated that (7*R*)-aryltetralin
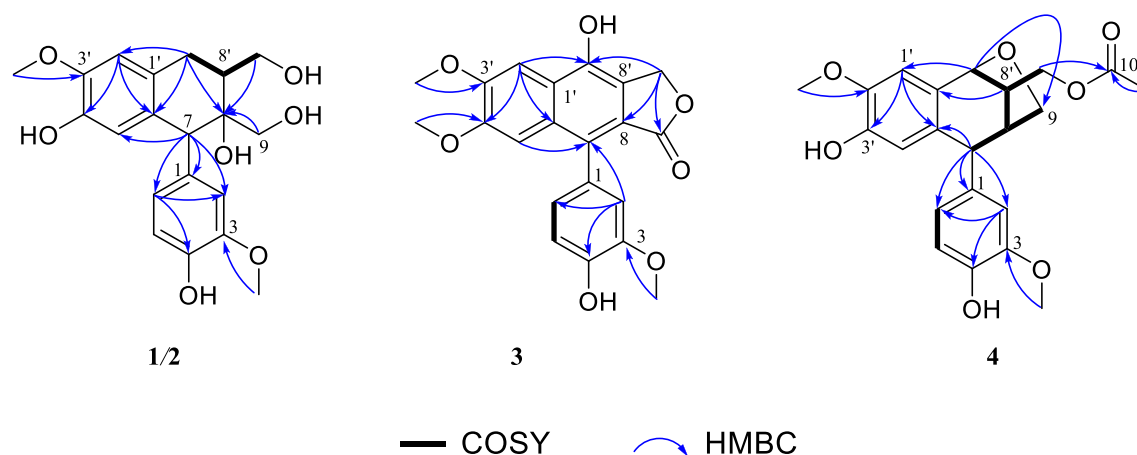
Fig. 2 ^{1}H–^{1}H COSY and key HMBC correlations of compounds 1–4. (Color need be used for this figure in print).
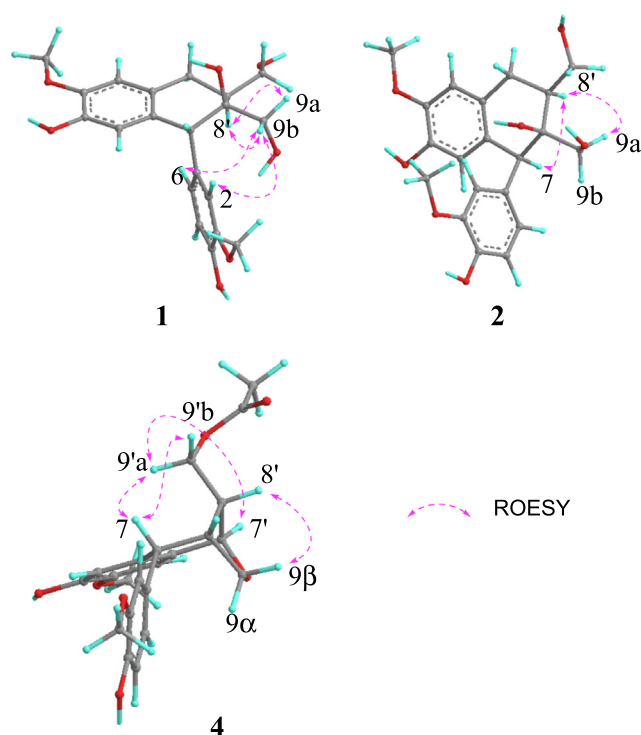
Fig. 3   Key ROESY correlations of compounds 1, 2 and 4. (Color need be used for this figure in print).

lignans displayed a first positive CE near 290 nm and a second negative CE near 270 nm, while the (7S)-configuration showed an opposite pattern. The experimental ECD spectrum of 1 (Fig. 4) showed CE patterns similar to those of (7R)-aryltetralin lignans, indicating that 1 had a (7R)-configuration. Meanwhile, the calculated ECD spectrum of the (7R,8S,8′S)-stereoisomer of 1 showed good agreement with the experimental ECD spectrum, which confirmed this deduction.

Saumedin B (2) displayed a molecular formula of $C_{20}H_{24}O_7$ as assigned by the sodium adduct ion $[M + Na]^+$ at m/z 399.1421 (calcd for $C_{20}H_{24}NaO_7$, 399.1414) in the (+)-HRESIMS. The IR spectrum of 2 showed a broad absorption band for hydroxy group at 3359 cm^{-1}, as well as absorption of

aromatic ring group at 1633, 1513, and 1035 cm^{-1}. Its ^{1}H and ^{13}C NMR spectra (Table 1) exhibited signals similar to those observed for 1, indicating that 2 was a diastereomer of 1, which was confirmed by the HMBC spectrum (Fig. 2) of 2.

The relative configuration of 2 was elucidated by the ROESY correlations (Fig. 3). The *syn* relative configuration between H-7 and H-8′ was deduced by the key cross-peak of H-7 and H-8′, which was arbitrarily assigned in an α-orientation. The β-orientation of OH-8 was assigned by the ROESY correlation between H-8′ and H-9a. Therefore, the relative configuration of 2 was determined to be 7S*,8S*,8′S*. The absolute configuration of C-7 was determined to be 7S, based on the evidence of a negative CE at 290 nm and a positive CE at 270 nm in the experimental ECD spectrum of 2. Furthermore, the calculated ECD spectrum of (7S,8S,8′S)-2 also showed a pattern similar to the experimental one (Fig. 4), supporting the assignment of the absolute configuration for 2 as 7S,8S,8′S.

Saumedin C (3) exhibited a molecular ion peak at m/z 383.1126 $[M + H]^+$ (calcd for $C_{21}H_{19}O_7$, 383.1125), corresponding to the molecular formula of $C_{21}H_{18}O_7$. The IR spectrum contained bands associated with hydroxy (3418 cm^{-1}), γ-lactone (1748 cm^{-1}) and aromatic ring (1602, 1515 and 1032 cm^{-1}) groups. The ^{1}H NMR spectrum (Table 1) of 3 showed the presence of a set of ABX systems at δ_H 6.90 (1H, d, $J = 1.8$, H-2), 6.93 (1H, d, $J = 8.1$, H-5), and 6.77 (1H, dd, $J = 8.0, 1.8$, H-6), two singlet aromatic protons at δ_H 7.68 (1H, s, H-2′), 7.10 (1H, s, H-5′), three methoxys at δ_H 3.84 (3H, s, 3-OMe), 4.01 (3H, s, 3′-OMe) and 3.72 (3H, s, 4′-OMe), meanwhile, a γ-lactone methylene group at δ_H 5.37 (2H, s, H-9′) was observed. The ^{13}C NMR spectrum of 3 revealed 21 carbon signals ascribable to 16 aromatic carbons (δ_C 101.9–152.3), a γ-lactone methylene at δ_C 68.2, one carbonyl carbon at δ_C 173.0, and three methoxy groups at δ_C 56.6, 56.3 and 56.0.

The ^{1}H and ^{13}C NMR spectral features suggested compound 3 had an arylnaphthalene lignan framework, which closely resembled that of detetrahydroconidendrin (Kawazoe et al., 2001). In comparing the ^{13}C NMR signals, a methoxy group located at C-4′ in compound 3 replaced the hydroxy group in detetrahydroconidendrin based on the HMBC correlations from OMe-4′ to C-4′, which was confirmed by the NOESY correlation between OMe-4′ and H-5′. In addition,
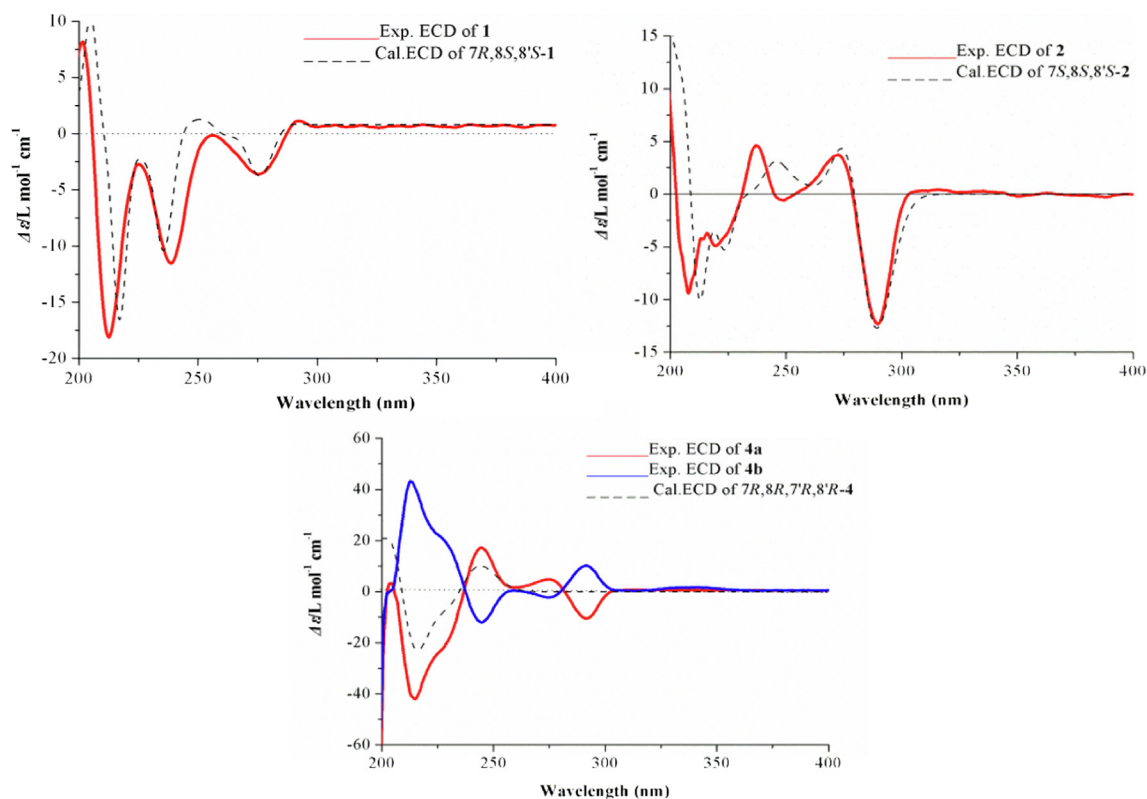
Fig. 4 Experimental and calculated ECD spectra of compounds 1, 2 and 4. (Color need be used for this figure in print).

C-7′ was strongly shifted downfield (δ_C 146.6) compared with that of detetrahydroconidendrin, suggesting that a hydroxy group was located at C-7′, which was in accordance with its molecular formula. Thus, compound **3** was elucidated and named saumedin C.

Saumedin D (**4**) possessed a molecular formula of $C_{22}H_{24}O_7$ on the basis of (+)-HRESIMS at *m/z* 423.1411 $[M + Na]^+$ (calcd for $C_{22}H_{24}NaO_7$, 423.1414) with 11 IHDs. Its IR spectrum showed absorption bands at 3422, 1736, 1602, 1514 and 1035 cm^{-1} due to hydroxy, carbonyl, and aromatic ring groups. The ^1H and ^{13}C NMR data (Table 1) of **4** showed the existence of one 1,2,4-trisubstituted aromatic ring at δ_H 6.61 (1H, d, *J* = 1.7, H-2), 6.86 (1H, d, *J* = 8.1, H-5), and 6.67 (1H, dd, *J* = 8.1, 1.7, H-6), one 1,2,4,5-tetrasubstituted benzene ring at δ_H 6.65 (1H, s, H-2′), 6.65 (1H, s, H-5′), two methoxy groups (δ_C 56.0, 56.1), two oxygenated methylenes (δ_C 62.1, 68.4), four methines (δ_C 44.5, 43.6 and 46.2, one oxygenated at δ_C 77.9). In addition, the signals at δ_H/δ_C 2.09 (3H, s)/20.9 and δ_C 171.0 indicated the presence of an acetoxy group. Two aromatic rings and one acetoxy group accounted for nine out of 11 IHDs, and the remaining two IHDs pointed to tetracyclic systems for compound **4**.

The above-mentioned evidence of **4** showed many similarities to those of **1**, suggesting that they had the same aryltetralin lignan skeleton, which was corroborated by the two dimensional (2D) NMR data. The main difference was that the hydroxy at C-9′ in **1** was acylated by an acetoxy group in **4**, as judged by the HMBC correlation (Fig. 2) from H$_2$-9′ to C-10′. Given that C-7′ (δ_C 77.9) and C-9 (δ_C 68.4) were dramatically shifted downfield compared to typical hydroxylated

carbons, an epoxy group was proposed between C-7′ and C-9. Moreover, the ^1H–^1H COSY correlations (Fig. 2) of H-7′/H-8′/H-8/H$_2$-9 and the HMBC correlation from H-7′ to C-9 confirmed the presence of a tetrahydrofuran ring D. Thus, the planar structure of **4** was elucidated to be a novel aryltetralin lignan with an oxygen bridge connecting C-7′ and C-9.

The relative stereochemistry of **4** was resolved by the ROESY analysis (Fig. 3). The ROESY correlation of H-7/H$_2$-9′ indicated that they were cofacial and assigned randomly as β-orientation, thus, H-8′ was α-orientation. The combination of the characteristics of the oxygen bridge and the ROESY correlation of H-8′ and H-9β revealed the β-orientation of H-7′ and H-8. Thus, the relative configuration of **4** was determined as 7*R**,8*R**,7′*R**,8′*R**.

The ECD spectrum was examined to identify the absolute configuration of **4**, but surprisingly, there was no obvious CE, which suggested the racemic nature of **4**. Therefore, a chiral HPLC analysis was carried out using a Waters 2695 liquid chromatography system on five parallel connected chiral columns (Column 1–5) with different proportion of mobile phase (A: *n*-hexane; B: isopropanol) (Fig. 5). Experimental results showed that compound **4** could be successfully separated on a Daicel IG chiral column (250 × 4.6 mm, S-5 μm) with 70:30 *v/v* (A/B) as mobile phase. Compounds (−)-**4a** and (+)-**4b** were successfully separated in a ratio of approximately 1:1 (Fig. 5), showing typical antipodal ECD curves (Fig. 4) and specific rotations of opposite sign. ECD calculations were carried out to establish their absolute configurations. The calculated ECD curve of (7*R*,8*R*,7′*R*,8′*R*)-form matched well with the experimental ECD spectrum of (−)-**4a** (Fig. 4), which
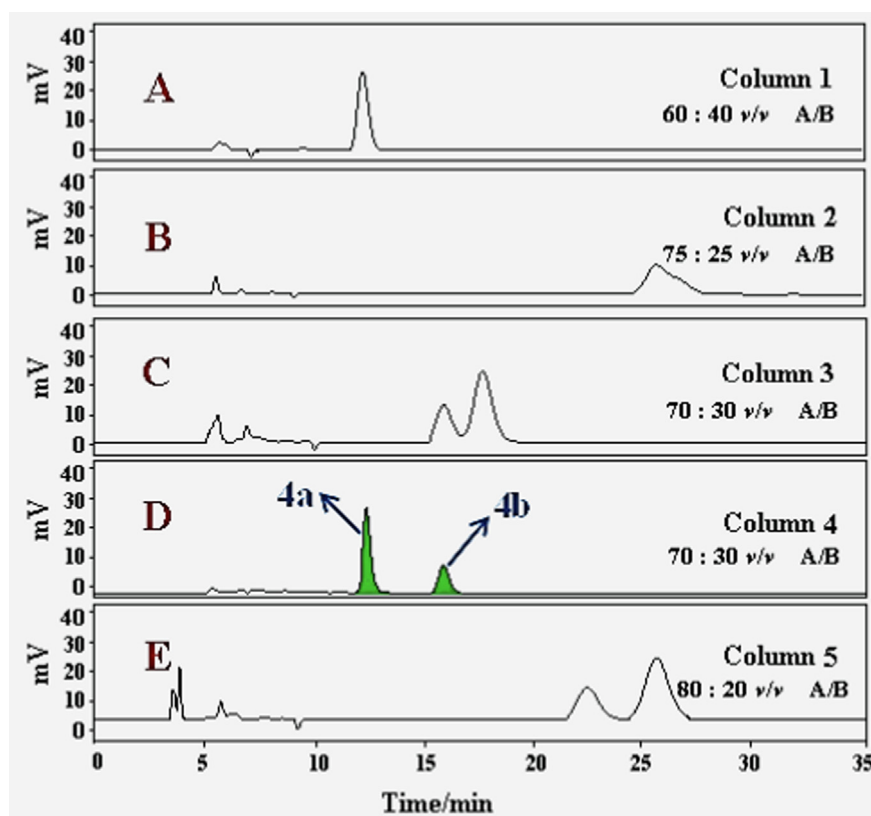
Fig. 5 Chiral HPLC analysis of 4a/4b on five parallel connected chiral columns (Column 1–5) with different proportion of mobile phase (A: *n*-hexane; B: isopropanol). (Color need be used for this figure in print).

allowed the assignment of the absolute configuration of (−)-**4a** as depicted $7R,8R,7'R,8'R$. Thus, (+)-**4b** was assigned as $7S,8S,7'S,8'S$.

Along with the new lignans, five known ones (−)-(α)-conidendrin monomethyl ether (Fischer et al., 2004) (**5**), (+)-isolariciresinol (Kwon et al., 2010) (**6**), burselignan (Jutiviboonsuk et al., 2005) (**7**), 5-methoxy-(+)- isolariciresinol (Pan et al., 2017) (**8**) and (+)-cycloolivil (Bai et al., 2015) (**9**) were also obtained and identified on the basis of spectroscopic analysis and comparison with the literature reported.

3.2. Anti-inflammatory effects

To measure the inhibitory effects of the isolated constituents against the inflammatory response, we used a cell-based screening bioassay to test the NO level in LPS-stimulated RAW 264.7 macrophages (Li et al., 2018). Cell viability assay in response to the purified constituent treatment was simultaneously determined to verify that the decrease of the NO level was not attributed to cell death. Quercetin was selected as a positive control with IC_{50} values of 15.9 ± 1.2 µM. The results revealed that there is no significant cytotoxicity under the measured concentration for all compounds. As showed in Table 2, compounds (−)-**4a** and **5** exerted the significant inhibition activities with IC_{50} values of 13.4 ± 1.5 and 15.7 ± 1.1 µM, respectively, which even exceeded the positive control drug quercetin. Compounds **2**, (+)-**4b**, **6** and **9** exhibited moderate inhibitory activities with IC_{50} values ranging from 19.7 ± 1.9 to 47.4 ± 3.1 µM.

Table 2 Inhibition of LPS-Induced NO Production.

compound	IC50 (µM)[a]	compound	IC50 (µM)
1	> 50	**5**	15.7 ± 1.1
2	21.0 ± 2.8	**6**	25.2 ± 2.0
3	> 50	**7**	> 50
4a	13.4 ± 1.5	**8**	> 50
4b	19.7 ± 1.9	**9**	47.4 ± 3.1
[b]quercetin	15.9 ± 1.2		

[a] Data expressed as the mean ± SD (n = 3).
[b] Positive control.

3.3. Molecular docking studies

The release of NO is mainly regulated by eNOS, nNOS, and iNOS, of which iNOS is vital to the release of NO and regulates the amount of NO in inflammatory processes (Lee et al., 2016). In order to explore the possible mechanism of inhibiting NO production, molecular docking studies were conducted to investigate the interaction between active compounds and iNOS proteins. The active compounds **2**, (−)-**4a**, (+)-**4b**, **5**, **6**, **9** and positive control drug quercetin were selected for molecular docking studies (Fig. 6). According to the docking results presented in Table 3, almost all active compounds had good affinities (docking scores < −7.0 kcal/mol) with iNOS proteins. Especially, compounds (−)−**4a** and **5** showed strong affinities with iNOS proteins, with affinities
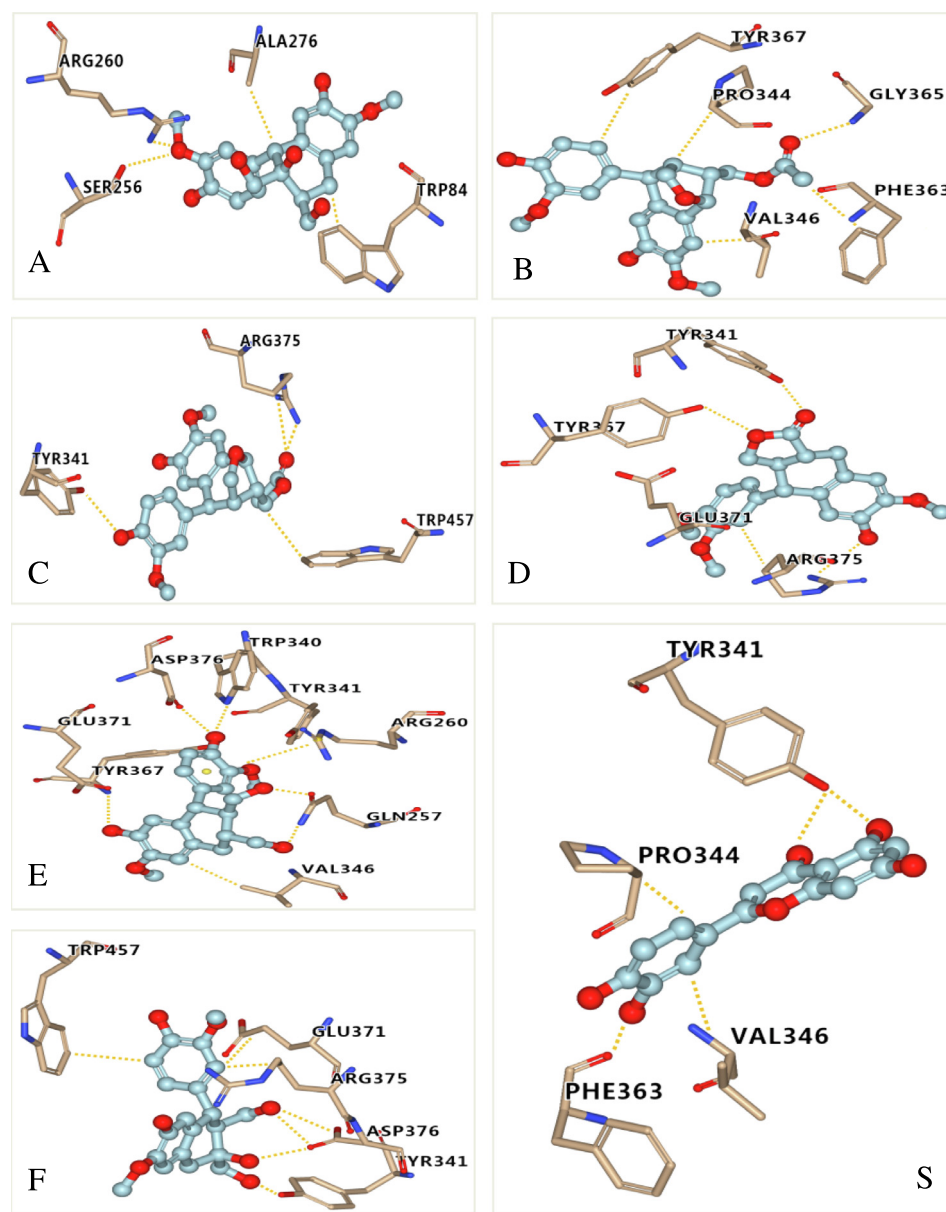
Fig. 6 Molecular docking simulations of compounds 2 (A), 4a (B), 4b (C), 5 (D), 6 (E), 9 (F) and quercetin (S) with iNOS. The hydrogen bonds interactions are shown by yellow dashed lines. (Color need be used for this figure in print).

Table 3 Docking results of active compounds with iNOS proteins.

compound	docking scores (kcal/mol)	hydrogen bond	hydrophobic interaction
2	−7.0	TRP340, TYR341, TYR367, ASP376, ARG382	PRO344, TRP457
4a	−7.6	GLY 365	PRO344, VAL346, PHE363, TYR367
4b	−7.4	ARG357, TYR341	TRP457
5	−7.7	TYR341, TYR367, ARG375	GLU371, ARG375
6	−6.9	GLN257, TRP340, TYR341 TYR367, GLU371, ASP376	VAL346 ARG260
9	−7.0	TYR341, ARG375, ASP376	TRP457, GLU371, ARG375
quercetin	−7.5	TYR341, PHE363	PRO344, VAL346

comparable to positive control drug quercetin (docking score = −7.5 kcal/mol), which was consistent with their stronger anti-inflammatory activities.

4. Conclusions

In summary, an investigation on the whole plants of S. medusa resulted in the isolation of five new arylnaphthalide lignans (1 − 4a/4b), including one pair of enantiomers (4a/4b), together with five known analogues (5–9). All compounds were isolated from S. medusa for the first time, among them, compound 5 was firstly separated from natural sources, and compounds 1–5, 7 and 8 were obtained from the genus Saussurea for the first time.

The anti-inflammatory effects on the production of NO by LPS-stimulated RAW 264.7 cells of all compounds were evaluated, and molecular docking study was employed to ascertain the binding mechanism of active compounds and iNOS proteins. This research revealed that arylnaphthalide lignans as possible chemical structural type in anti-inflammatory activities, which might give an insight for the skeleton reference of the related drug design. To the best of our knowledge, this was the first comprehensive report on the arylnaphthalide lignan compounds of S. medusa and their anti-inflammatory activities. Furthermore, this study provided scientific background for further understanding the chemical composition and biological functions of S. medusa.

Declaration of Competing Interest

The authors declare that they have no known competing financial interests or personal relationships that could have appeared to influence the work reported in this paper.

Acknowledgements

Appendix A. Supplementary material

Supplementary data to this article can be found online at https://doi.org/10.1016/j.arabjc.2022.104155.

References

Aktan, F., 2004. iNOS-mediated nitric oxide production and its regulation. Life Sci. 75, 639–653. https://doi.org/10.1016/j.lfs.2003.10.042.

Ayres, D.C., Loike, J.D., 1990. Lignans: Chemical, biological and clinical properties (Chemistry and Pharmacology of Natural Products). Cambridge University Press, Cambridge 247−268. https://doi.org/10.1016/0306-3623(91)90258-8

Azam, F., Medapati, V., Thangavel, N., Shrivastava, A.K., Mohan, G., 2012. Structure-based design, synthesis and molecular modeling studies of thiazolyl urea derivatives as novel anti-Parkinsonian agents. Med. Chem. 8, 1057–1068. https://doi.org/10.2174/157340612804075034.

Bai, M.M., Shi, W., Tian, J.M., Lei, M., Kim, Y.H., Sun, Y.N., Kim, J.H., Gao, J.M., 2015. Soluble epoxide hydrolase inhibitory and anti-inflammatory components from the Leaves of Eucommia ulmoides Oliver (Duzhong). J. Agric. Food Chem. 63, 2198–2205. https://doi.org/10.1021/acs.jafc.5b00055.

Bruhn, T., Schaumlöffel, A., Hemberger, Y., Bringmann, G., 2013. SpecDis: quantifying the comparison of calculated and experimental electronic circular dichroism spectra. Chirality 25, 243–249. https://doi.org/10.1002/chir.22138.

Cuong, T.D., Hung, T.M., Kim, J.C., Kim, E.H., Woo, M.H., Choi, J. S., Lee, J.H., Min, B.S., 2012. Phenolic compounds from Caesalpinia sappan heartwood and their anti-inflammatory activity. J. Nat. Prod. 75 (12), 2069–2075. https://doi.org/10.1021/np3003673.

Day, S.H., Chiu, N.Y., Tsao, L.T., Wang, J.P., Lin, C.N., 2000. New lignan glycosides with potent antiinflammatory effect, isolated from Justicia ciliata. J. Nat. Prod. 63 (11), 1560–1562. https://doi.org/10.1021/np000191j.

Duan, H.Q., Takaishi, Y., Momota, H., Ohmoto, Y., Taki, T., 2002. Immunosuppressive constituents from Saussurea medusa. Phytochem. 59, 85–90. https://doi.org/10.1016/S0031-9422(01)00429-0.

Fan, J.Y., Chen, H.B., Zhu, L., Chen, H.L., Zhao, Z.Z., Tao, Y., 2015. Saussurea medusa, source of the medicinal herb snow lotus: a review of its botany, phytochemistry, pharmacology and toxicology. Phytochem. Rev. 14, 353–366. https://doi.org/10.1007/s11101-015-9408-2.

Fan, C.Q., Yue, J.M., 2003. Biologically active phenols from Saussurea medusa. Bioorg. Med. Chem. 11, 703–708. https://doi.org/10.1016/S0968-0896(02)00470-4.

Fischer, J., Reynolds, A.J., Sharp, L.A., Sherburn, M.S., 2004. Radical carboxyarylation approach to lignans. total synthesis of (-)-arctigenin, (-)-matairesinol, and related natural products. Org. Lett. 6 (9), 1345–1348. https://doi.org/10.1021/ol049878b.

Frisch, M.J., Trucks, G.W., Schlegel, H.B., Scuseria, G.E., Robb, M. A., Cheeseman, J.R., Scalmani, G., Barone, B.V., Petersson, G.A., Nakatsuji, H., Li, X., Caricato, M., Marenich, A.V., Bloino, J., Janesko, B.G., Gomperts, R., Mennucci, B., Hratchian, H.P., Ortiz, J.V., Izmaylov, A.F., Sonnenberg, J.L., Williams, D., Ding, F., Lipparini, F., Egidi, F., Goings, J., Peng, B., Petrone, A., Henderson, T., Ranasinghe, D., Zakrzewski, V.G., Gao, J., Rega, N., Zheng, G., Liang, W., Hada, M., Ehara, M., Toyota, K., Fukuda, R., Hasegawa, J., Ishida, M., Nakajima, T., Honda, Y., Kitao, O., Nakai, H., Vreven, T., Throssell, K., Peralta,; J.E., Ogliaro, F., Bearpark, M.J., Heyd, J.J., Brothers, E.N., Kudin, K. N., Staroverov, V.N., Keith, T.A., Kobayashi, R., Normand, J., Raghavachari, K., Rendell, A.P., Burant, J.C., Iyengar, S.S., Tomasi, J., Cossi, M., Millam, J.M., Klene, M., Adamo, C., Cammi, R., Ochterski, J.W., Martin, R.L., Morokuma, K., Farkas, O., Foresman, J.B., Fox, D.J., 2016. Gaussian 16 Rev. A.03, Wallingford, CT.

Gertsch, J., Tobler, R.T., Brun, R., Sticher, O., Heilmann, J., 2003. Antifungal, antiprotozoal, cytotoxic and piscicidal properties of Justicidin B and a new arylnaphthalide lignan from Phyllanthus piscatorum. Planta Med. 69, 420–424. https://doi.org/10.1055/s-2003-39706.

Guzik, T.J., Korbut, R., Adamek-Guzik, T., 2003. Nitric oxide and superoxide in inflammation and immune regulation. J. Physiol. Pharmacol. 54, 469–487. https://doi.org/10.1152/jn.00313.2003.

Hagerling, C., Casbon, A.J., Werb, Z., 2015. Balancing the innate immune system in tumor development. Trends Cell Biol. 25, 214–220. https://doi.org/10.1016/j.tcb.2014.11.001.

Harder, E., Damm, W., Maple, J., Wu, C.J., Reboul, M., Xiang, J.Y., Wang, L.L., Lupyan, D., Dahlgren, M.K., Knight, J.L., Kaus, J. W., Cerutti, D., Krilov, G., Jorgensen, W.L., Abel, R., Friesner, R. A., 2015. OPLS3: a force field providing broad coverage of drug-

like small molecules and proteins. J. Chem. Theory Comput. 12, 281–296. https://doi.org/10.1021/acs.jctc.5b00864.

Hussain, M.S., Azam, F., Eldarrat, H.A., Haque, A., Khalid, M., Hassan, M.Z., Ali, M., Arif, M., Ahmad, I., Zaman, G., Alabdallah, N.M., Saeed, M., 2022. Structural, functional, molecular, and biological evaluation of novel triterpenoids isolated from *Helichrysum stoechas* (L.) Moench. collected from mediterranean sea bank: Misurata-libya. Arab. J. Chem. 15,. https://doi.org/10.1016/j.arabjc.2022.103818 103818.

Jutiviboonsuk, A., Zhang, H.J., Tan, G.T., Ma, C.Y., Hung, N.V., Cuong, N.M., Bunyapraphatsara, N., Soejarto, D.D., Fong, H.H.S., 2005. Bioactive constituents from roots of *Bursera tonkinensis*. Phytochem. 66, 2745–2751. https://doi.org/10.1016/j.phytochem.2005.09.025.

Kawazoe, K., Yutani, A., Tamemoto, K., Yuasa, S., Shibata, H., Higuti, T., Takaishi, Y., 2001. Phenylnaphthalene compounds from the subterranean part of *vitex rotundifolia* and their antibacterial activity against methicillin-resistant *staphylococcus aureus*. J. Nat. Prod. 64, 588–591. https://doi.org/10.1021/np000307b.

Kwon, J.H., Kim, J.H., Choi, S.E., Park, K.H., Lee, M.W., 2010. Inhibitory effects of phenolic compounds from needles of *pinus densiflora* on nitric oxide and PGE$_2$ production. Arch. Pharm. Res. 33 (12), 2011–2016. https://doi.org/10.1007/s12272-010-1217-y.

Lee, S.R., Lee, S., Moon, E., Park, H.J., Park, H.B., Kim, K.H., 2016. Bioactivity-guided isolation of anti-inflammatory triterpenoids from the sclerotia of *Poria cocos* using LPS-stimulated Raw264.7 cells. Bioorg. Chem. 70, 94–99. https://doi.org/10.1016/j.bioorg.2016.11.012.

Li, Y.R., Fu, C.S., Yang, W.J., Wang, X.L., Feng, D., Wang, X.N., Ren, D.M., Lou, H.X., Shen, T., 2018. Investigation of constituents from *Cinnamomum camphora* (L.) J. Presl and evaluation of their anti-inflammatory properties in lipopolysaccharide-stimulated RAW 264.7 macrophages. J. Ethnopharmacol. 221, 37–47. https://doi.org/10.1016/j.jep.2018.04.017.

Pan, Y.P., Ye, J., Zhang, Y., Jin, H.Z., 2017. Chemical constituents of *Hedyotis uncinella*. Chem. Nat. Compd. 53 (4), 738–739. https://doi.org/10.1007/s10600-017-2104-2.

Pescitelli, G., Bruhn, T., 2016. Good computational practice in the assignment of absolute configurations by TDDFT calculations of ECD spectra. Chirality 28, 466–474. https://doi.org/10.1002/chir.22652.

Selmi, C., Generali, E., Massarotti, M., Bianchi, G., Sciré, C.A., 2014. New treatments for inflammatory rheumatic disease. Immunol. Res. 60, 277–288. https://doi:org/10.1007/s12026-014-8565-5.

Su, X.M., Federoff, H.J., 2014. Immune responses in Parkinson's disease: Interplay between central and peripheral immune systems. Biomed. Res. Int. 275178, 1–9. https://doi.org/10.1155/2014/275178.

Sun, Y.J., Wang, J.M., Chen, H., Hua, H.M., 2013. Advances in studies on aryltetralin lactone lignans. China J. Chin. Mater. Med. 38 (13), 2051–2059. https://doi.org/10.4268/cjcmm20131303.

Tran, T.D., Pham, N.B., Booth, R., Forster, P.I., Quinn, R.J., 2016. Lignans from the Australian endemic plant *Austrobaileya scandens*. J. Nat. Prod. 79 (6), 1514–1523. https://doi.org/10.1021/acs.jnatprod.5b00988.

Tuchinda, P., Kumkao, A., Pohmakotr, M., Sophasan, S., Santisuk, T., Reutrakul, V., 2005. Cytotoxic arylnaphthalide lignan glycosides from the aerial parts of *Phyllanthus taxodiifolius*. Planta Med. 72, 60–62. https://doi.org/10.1055/s-2005-873141.

Wang, Z.Q., Palaniappan, S., Affendi, R., Ali, R., 2014. Inflammatory bowel disease-related colorectal cancer in the Asia-pacific region: past, present, and future. Intest. Res. 12 (3), 194–204. https://doi.org/10.5217/ir.2014.12.3.194.

Xie, H.H., Wang, T., Matsuda, H., Morikawa, T., Yoshikawa, M., Tani, T., 2005. Bioactive constituents from Chinese natural medicines. XV. inhibitory effect on aldose reductase and structures of Saussureosides A and B from *Saussurea medusa*. Chem. Pharm. Bull. 53 (11), 1416–1422. https://doi.org/10.1002/chin.200617192.

Yu, R.X., Jiang, L., Mei, L.J., Tao, Y.D., Yu, R.T., Xia, X.C., 2019. Anti-inflammatory effects of alcohol extract from *Saussurea medusa* Maxim against lipopolysaccharides-induced acute lung injury mice. Int. J. Clin. Exp. Medic. Res. 3 (4), 112–118.

Zhang, Y., Liu, J.Z., Wang, M.Y., Sun, C.J., Li, X.B., 2019. Five new compounds from *Hosta plantaginea* flowers and their anti-inflammatory activities. Bioorg. Chem. 95,. https://doi.org/10.1016/j.bioorg.2019.103494 103494.